2014 IEEE International Conference on Robotics & Automation (ICRA)
Hong Kong Convention and Exhibition Center
May 31 - June 7, 2014. Hong Kong, China

A Method for Capturing the Tacit Knowledge in the Surface Finishing Skill by Demonstration for Programming a Robot*

Charles. W. X. Ng, Kelvin. H. K. Chan, W. K. Teo, I-Ming. Chen

***Abstract*—This paper describes a methodology for capturing the tacit knowledge of the manual grinding and polishing process. Key Process Variables (KPVs) i.e. contact force, tool path, feed rate, etc. of the manual operator performing the task are captured with a 'sensorised' hand-held belt grinder, while the changes to the work-piece geometry is captured using a 3-D laser scanner. These KPVs are fed into an analytical material removal model to generate a material removal profile, which can then be calibrated using the actual material removed determined from the manual surface finishing process. The skill of the surface finishing skill is encapsulated in this material removal model and reduces the need for costly robotic Design of Experiment (DoE) trials with test coupons to develop empirical material removal models. Parts from the production process require different processing variables, but the common objective is to generate various material removal maps in order to manufacture a part of a desired form and dimension. The metal removal rate (MRR) model could then be utilized by the industrial robot to determine suitable polishing parameters to accomplish the polishing task. The characteristics of the skilled worker's captured motions can then be extracted and used for optimization of the industrial robot polishing tool path.**

I. Introduction

Many surface finishing tasks such as the grinding of free-form surfaces to tolerance are still performed manually with a hand-held flexible belt grinder. Parts that are sent for surface finishing may have slight variations in their initial geometry. Thus, for every part to achieve dimensional conformance and meet the required surface roughness, different grinding parameters and tool paths have to be used for each part or work-piece. The manual operator has a wealth of experience and can adapt to variations in the inputs and determine suitable grinding tool paths and parameters to produce the desired output, which is a part that is within tolerance. However, these surface finishing tasks are potentially hazardous to health if too much metallic dust is inhaled when the proper protective equipment is not used. Furthermore, manual processes may be prone to human errors, resulting in the part having to be scrapped or sent for rework. Therefore, it is desirable for these manual surface finishing tasks to be automated with an industrial robot.

One of the first steps in the conversion of a manual to automated process is the development of an empirical material removal model for the work-piece to be finished. A flat test piece coupon may be first used to determine the parameters required for constant material removal of a certain thickness. Next, the parameters will be optimized for constant material removal over the actual work-piece geometry by conducting trials on a test piece that represents the geometry of the work-piece. The differences in the contact pressure due to the curvatures of the work-piece has to be accounted for by tweaking variables such as the step over distance of the tool path and the feed rate. The disadvantage of this approach is that it is time consuming and also an expensive process. Many DoE trials involving robot programming and consumables such as test coupons and abrasive belts have to be completed in order to obtain the relationship between the Key Process Variables (KPVs) and Material Removal Rate (MRR) [1].

This paper presents a novel method to capture the relationship between the KPVs and the MRR accurately without the need for costly robotic trials and DoE. The flexible hand-held belt grinder used by the manual operators for the surface finishing process is integrated with sensors and infra-red markers to capture the contact force, feed rate and tool paths. The capturing process can be carried out while the operator performs the surface finishing process on the production shop floor by utilizing the 'sensorized' belt grinder. A 3D laser scanner would also be used to capture the changes in the work-piece geometry when the operator stops to inspect the part. The data collected from the 'sensorized' tool would be fed into an analytical material removal model [2-4] to calculate a material removal map. The experimental material removal map can then be generated from the 3D data captured by the laser scanner of the actual manual process. The analytical model can then be calibrated by fitting the predicted material removal map generated by the analytical model against the actual material removal map captured from the manual process.

With the captured data of the manual operator converted to the form of a model relating the KPVs to the MRR, the robot programmer can easily use this information to decide the required parameters based on the desired amount of material to be removed. This eliminates the need for guess work when deciding the required parameters and produce cost savings on the purchase of consumables since robotic trials on flat or curved test coupons do not need to be carried out in order to develop the material removal model. The relationship between the depth of material removed and the surface finishing KPVs can be obtained directly from the manual operator during the production process. This information was previously lost as there was no method of capturing the KPVs of the manual surface finishing process.

*Research supported by Rolls-Royce and Singapore EDB IPP Program.

W. X. Ng is with the Nanyang Technological University, Singapore (phone: 65-240-3157; e-mail: ngwu0003@e.ntu.edu.sg).

W. K. Teo and H. K. Chan are with Rolls-Royce Singapore (email: wee.teo@rolls-royce.com and kelvin.chan@rolls-royce.com)

I. M. Chen, is an Associate Professor with the Nanyang Technological University, Singapore. (e-mail: michen@ntu.edu.sg).

Previous work on optimizing path planning for robotic belt grinding do not take into account the tacit knowledge of the manual operator and are based more on the experience of the robot programmers [5, 6]. Thus, this paper also presents a method of using the captured manual tool path using a 'sensorized' tool to optimize the method of translating a manual to robotic process. This is done by extracting features from multiple demonstrations of the manual motions and converting it to its equivalent robotic KPVs (step-over distance, coverage area, etc), while the theoretical model can be used to calculate the required parameters in order to achieve the desired material removal map for each work-piece, since there may be variations in the parts coming through the production process. Porting the manual tool path trajectories and contact forces directly to the robot will not guarantee that the work-piece geometry and surface finish will be within tolerance. This is because the operator would vary the tool path in each cycle to adapt to the requirements of the individual work-piece based on the information gathered from his senses. On the other hand, the robot is blind and does not have a closed loop feedback system.

II. Capturing the KPVs of the Manual Process

A. Capture Equipment and System

Sensors for measuring the KPVs of the material removal process will have to be integrated with the hand-held belt grinder used by the manual polisher. The mounting side of the 6 degree of freedom ATI force/torque sensor is attached to the end of the belt grinder's contact arm (Figure 1).

Figure 1.Sensorized Tool

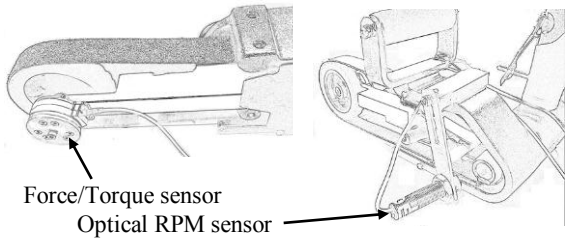

A shaft is attached to the end effector attachment side of the force/torque sensor, where the contact wheel is attached. Active LEDs are attached to the belt grinder and work-piece to capture the position, velocity and orientation of the Tool Centre Point (TCP) using a Nikon K600 optical CMM. A tachometer is also integrated to measure the spindle speed of the contact wheel.

Figure 2. Handheld 3D laser from Nikon (K-Scan MMDx)

www.nikonmetrology.com

A laser scanner is also required to sample the 3 dimensional surface of the work-piece after each grinding correction cycle of the manual operator. The laser scanner (Figure 2) is also tracked by the Nikon K600 optical CMM to reconstruct the point cloud of the surface.

B. Determining the Contact Force and TCP

The contact force of the belt grinder on the surface of the work-piece can be modeled as a point force acting on the shaft at a location in the centre of the bearing (Figure 3). At the origin of the ATI sensor, this point force will be equivalent to a force of the same magnitude and direction, as well as a moment due to the offset of the force from the origin.

Figure 3. Calculation of Contact Force

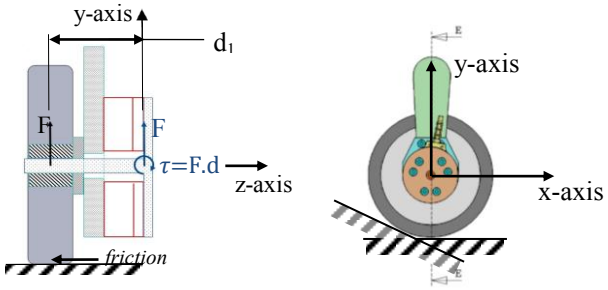

The friction force which is a fraction of the contact force F, applied on the surface of the workpiece is assumed to be small compared to the contact force mesured by the ATI sensor. In calculating the contact force, it is also assumed that the contact wheel is normal to the surface of the workpiece. Thus, the contact force is

$$F_n = \sqrt{F_x{}^2 + F_y{}^2}. \quad (1)$$

This can be validated by using the position data of the belt grinder Tool Centre Point (TCP) and workpiece captured with the optical infra-red cameras to visualise the manual tool path. Thus the approach vector of the belt grinder can be compared with the actual normal vector to the workpiece surface. In Figure 4, the red vectors show the approach angle of the tool while the blue vectors indicate the normal of the workpiece surface at the tool contact point.

Figure 4. Visualization of captured TCP

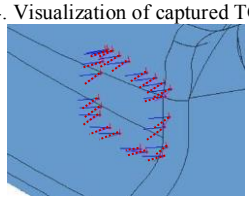

The tool centre point on the belt grinder is not fixed but can be at any position along the the circumference of the contact wheel. Figure 3 shows the xy-axes plane of the ATI sensor. To determine the contact point along the circumference of the wheel, the magnitude of the force along the x and y axes are added vectorially at every time step, where the angle direction of the force in the xy plane corresponds to the position of the contact point along the wheel circumference. Thus, the angle of the force direction is

$$\theta_{F_n} = tan^{-1}(\frac{F_y}{F_x}). \quad (2)$$

It is important to note the sign of the force vectors to determine the quadrant where the angle direction lies.

$$TCP_x = R\cos(\theta_{F_n}), \quad (3)$$

$$TCP_y = R\sin(\theta_{F_n}), \quad (4)$$

where R is the radius of the contact wheel. This is then used to calculate the coordinate point where the tool is in contact with the workpiece surface. With the other end of the vector being the coordinate point of the contact wheel shaft centre, the approach vector is constructed. Let position of the hand held grinder tool relative to the global origin be represented by the homogeneous transformation matrice H_T^o. The homogenous matrice representing the position and orientation of the workpiece relative to the global origin is H_W^o. Thus, the homogeneous matrice of the tool relative to the workpiece,

$$H_T^W = H_o^W\, H_T^o. \quad (5)$$

Position/Orientation of the origin of the integrated force/torque sensor relative to the workpiece becomes,

$$H_S^W = H_T^W\, H_S^T, \quad (6)$$

where H_S^T is the homogenous transformation matrice between the origin of the LED infra-red markers and the force/torque sensor origin. Location of the instantaneous contact point between the tool and the workpiece is

$$H_{TCP}^W = H_S^W \begin{pmatrix} 1 & 0 & 0 & TCP_x \\ 0 & 1 & 0 & TCP_y \\ 0 & 0 & 1 & 0 \\ 0 & 0 & 0 & 1 \end{pmatrix}, \quad (7)$$

where TCP_x and TCP_y are obtained from (3) and (4). Hence, the 3-by-1 approach direction of the instantaneous tool centre point is calculated by subtracting the position component of $H_{TCP}^W$and H_S^W, followed by dividing by the norm of the distance between them. The translation component of the entire collection of H_{TCP}^W homogenous matrices represent the tool path of the manual operator.

C. Calculating the Surface Finishing KPVs and Trajectories

The target points of the manual operator's surface finishing strategy have to be converted into KPVs which can be utilized by the robot programmer in the development of the automation strategy. The KPVs that need to be calculated are the cutting speed, feed rate, contact force and the orientation of the wheel head relative to the tool path direction. The cutting speed can be estimated from the specifications of the pneumatic belt grinder. Alternatively, an rpm sensor can be attached to the belt grinder to record the instantaneous cutting speed. The time discretized feed rate is calculated based on the distance between each target point sampled and the interval sample time. The contact force magnitude of the manual strategy is calculated from the forces in the x and y axes recorded by the ATI sensor. To calculate the orientation angle of the belt polisher, the tangent to the tool path (where the tool path is represented by the collection of discretized tool contact points) is first calculated for every target point. The orientation of the belt grinder is directly determined from the optical infra-red camera tracker. Lastly, the angle between the orientation of the contact wheel and the tool path direction is then calculated with a dot product.

III. Calibration of the Material Removal Model

A. Simulating the Human Environment Interaction

The environment is the work-piece, while the interaction refers to surface finishing. In order to generalize the captured data from the manual surface finishing process, a theoretical material removal model is utilized to simulate the material removal map based on the captured KPVs. This is because the captured data alone may be of limited use, as the work-pieces in the production process may vary from part to part. Hence, the parameters used by the manual operator, such as the forces, feed rate or number of passes for a certain part will not be applicable to the next one. In addition, the tool path captured may have subtle techniques used by the operator that are not replicable by the robot.

Figure 5. Modeling of Contact Pressure

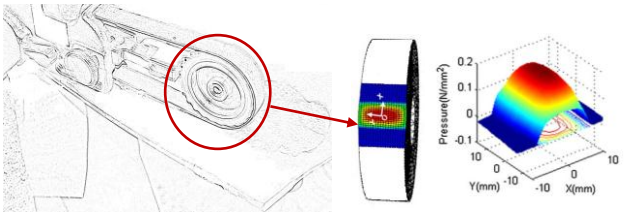

Therefore, a theoretical or analytical material removal model [3, 4, 7] is a very suitable tool to interpret the captured KPVs in terms of a material removal map and present the relationship between the KPVs captured from the manual operator and the amount or depth of material removed per unit length, which is the tool impression function $w_{h/l}$

This way, the programmer would be able to use the relationship between the KPVs and material removal to program the robot as it is in the form of robot parameters (i.e. feed-rate, contact force etc).

DoE trials which are used currently to determine the relation between the robotic KPVs and MRR may also be eliminated. These trials may be costly as they require time to program and to set up the robot tool path and robot cell before linishing of the work-pieces are carried out, as well as money to purchase consumables such as test coupons, coolant and abrasive belts. Furthermore, time is needed to measure the depth of material removed using a GOM ATOS 3D scanner (www.gom.com) or ultrasonic sensor.

B. The Theoretical Material Removal Map

Based on the Hertzian contact stress model to simulate the pressure distribution (Figure 5), the MRR model can be developed based on the Archard wear law to calculate the tool impression function, which is the depth of material removed from the surface for one unit time of tool dwell. According to the Hertzian model, the contact area between the part and the polishing tool is an ellipse that depends on

the local radius of curvature of the part, assuming a constant compressive force. In order to model the material removal over the three dimensional free-form surfaces, the tool impression function is convoluted with the captured tool path of the manual operator [3]. Some results of this model are presented in Figure 6, where the predicted material removal maps of two robotic paths are shown. The model will be similarly applied to the human tool paths captured.

Figure 6. Material removal map validation.

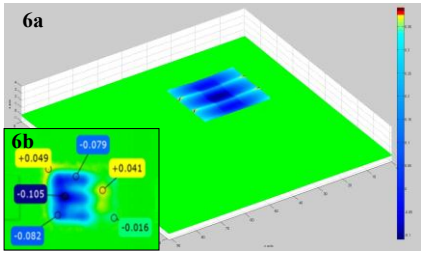

Figure 6a shows the actual shape of the linished surface measured by a GOM 3D scanner. Figure 6b shows the predicted final shape of the linished surface with the same input KPVs as the actual trial carried out. The general pattern can be observed to be similar, however, differences arises in the peak to valley heights. KPVs of the surface finishing process are fed into the theoretical model to generate the material removal map for a free-form surface shown in Figure 7, where the colors indicate different depths of material removed.

Figure 7. Material removal maps for a convex free-form surface, given the robotic surface finishing KPVs.

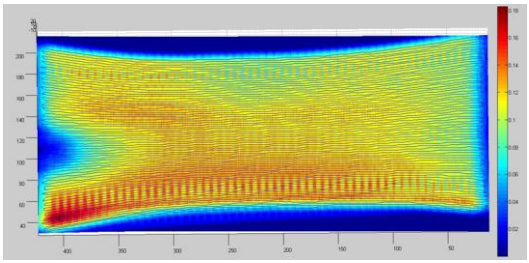

The tool path is first obtained from a CAD/CAM software comprising of a list of xyz coordinates. The first step is to use these points to fit a surface given the x, y and z points using the *gridfit* Matlab function. This returns a 2 dimensional array, $G_{n\times m}$ of values corresponding to the height map of the fitted surface. Next, the maximum and minimum principal curvatures are calculated using the *surfature* Matlab function. The list of tool paths are next rounded to the nearest discretized position on the surface. The discretized tool paths, $Toolpaths_{k\times 1}$ (k is the number of tool path xyz coordinates) is then compared with the x and y array values of $G_{n\times m}$, x_{nodes} from 1 to n, and y_{nodes} from 1 to m. The tool impression function, $w_{h/l}$ can be calculated for every tool path coordinate point using the equation

$$w_i(x,y) = \frac{k_{abr}\times V\times p_i(x,y)}{H_v\times V_f}\times Dist_i, for\ i = 1\ to\ k. \quad (8)$$

Where the contact pressure,

$$p_i(x,y) = -p_0\sqrt{1-\left(\frac{x}{a_i}\right)^2-\left(\frac{y}{b_i}\right)^2}\cdot(1+c(y)), \quad (9)$$

$$c(y) = R_*^k\cdot polynomial\left(\left|\frac{2y}{W}\right|\right), \quad (10)$$

and V is the nominal spindle speed, V_f is the feed speed of the tool, H_v is the hardness of the part surface, K_{abr} the cutting parameter of the abrasive belt, *Dist* is the distance between two coordinate points, a and b are the semi-major and minor axes of the contact ellipse which depends on the radius of curvature of the work piece. The material removal map can be determined by a convolution of the depth map $w_i$with the discretized tool path points.

C. Capturing the Experimental Material Removal Map

The experimental material removal map can be captured using a Nikon K-Scan MMDx walkaround scanning. The laser scanner is tracked by the Nikon K600 optical CMM, which enables three dimensional CAD data of the work-piece surface to be measured. The manual operator's surface finishing strategy consists of multiple correction cycles; each cycle involves grinding of the surface of the work-piece and inspecting the surface visually and by touch. This forms a closed loop system, ensuring that the final work-piece will be within dimensional tolerance. In each correction cycle, the Nikon K600 optical CMM will track the position of the hand-held belt grinder used by the operator. The K-Scan MMDx, which is also tracked by the Nikon K600, will be used to sample the surface of the work-piece each time the operator stops to inspect the surface. The difference between the surfaces scanned between each correction cycle can be determined using Polyworks™ software to derive the material removal map.

D. Determining the Unknown Parameters

The theoretical material removal model has several unknown parameters, such as a value K_{abr} to represent the cutting effectiveness of the abrasive belt, or the effect of the contact wheel serrations (land to groove ratio, serration angle) on the contact pressure. The experimental material removal map captured with the laser scanner can be used to calibrate the predicted material removal map generated from the theoretical model by choosing values of these unknown parameters heuristically such that the two material removal maps will be aligned. With the unknown parameters obtained, the material removal model can be used for other work-pieces which may have different geometries.

As a consequence, the belt wear can also be determined as it is related to the cutting effectiveness constant in the theoretical model. At the end of each correction cycle, variable parameters such as the cutting effectiveness can be determined by re-calibrating the theoretical material removal map with the experimental map. This is due to the belt wear, as the cutting grains on the belt become blunt, the cutting effectiveness would fall, resulting in a corresponding drop in this parameter. By assuming a linear relationship between the length of the tool path and the cutting effectiveness constant, the rate of the belt wear can be determined between each calibration.

IV. Robot Teaching Tool for Surface Finishing

A. Differences between the Manual and Robotic Strategy

In the manual surface finishing strategy, there are multiple correction cycles. The manual operator corrects for the form errors in the work-piece by adjusting the number of grinding passes over the surface until the error is within the acceptable range. On the other hand, the robotic strategy for correcting the form errors over the surface of the work-piece typically involves only one pass, while the feed speed or contact force can be adjusted to remove different depths of material spatially. This is the fundamental difference between the manual and robotic strategy, and is a consequence of the different capabilities of the robot and a human. Because the robot typically uses one pass, the contact force applied on the work-piece would be significantly greater than those applied by the manual operator. The life of the abrasive belt can be extended on the robotic process as greater forces can be achieved in order to produce the same rate of material removal.

Figure 8. Program to port motions from a human demonstration to robotic system

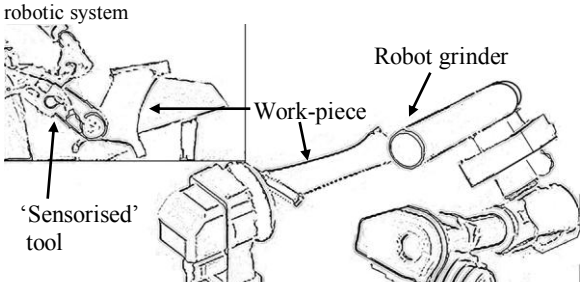

The industrial robot is able to control the feed rate and position of the belt-grinder finely while the manual operator can never reach the same accuracy and repeatability. The operating force of the robot is also significantly higher than the maximum forces the manual operator can attain. However, the manual operator is a lot more dexterous than the industrial robot. Errors arise when the robot transitions from position to force control, as well as when it disengages the surface and lifts off. In addition, it takes time to transition from one control scheme to another. Hence, it is impractical to have the robot program that mimics the exact manual strategy of having multiple but discontinuous passes, as it would involve many control transitions. It is also impractical to directly implement the organic motions of the manual operator into the robot program, as the robot has different mass and inertia properties from the human. As a result, the dynamic motion of the robot may not be similar to that of the manual operator performing the manual tool path but jerky and undesirable. Thus, a local regression using weighted linear least squares smoothening of the captured tool path was performed before porting the simple grinding tool path to the robot (Figure 8).

B. Benefits of Modeling the Manual Surface Finishing with a Theoretical Material Removal Model

In order to utilize the data captured from the manual surface finishing strategy to program an industrial robot, the manual surface finishing process has to be modeled for a number of reasons. Firstly, the length of the handheld grinder's abrasive belt used by the manual operator is significantly shorter than that of the grinder attached to the robot end-effector. Thus, the rate of belt wear will be different, and even if the same parameters are ported over, there would not be a similar result observed, and the work piece will not have the desired geometry or finish. Furthermore, differences between the size and properties of the handheld grinder and robot head grinder's contact wheel limits the use of the captured data from the manual process in the robotic surface finishing program.

Hence, a method to correct for these differences is needed in order for the captured manual data to be applicable in the robotic environment. Therefore, the material removal model was introduced to account for the difference in belt wear and contact wheel diameter. The contact pressure from the different contact wheel sizes can be calculated, thus other KPVs such as the contact force can be adjusted to maintain the same contact pressure from the manual to robotic tool path. Also, the change in belt abrasiveness can be quantified through the use of a parameter in the theoretical material removal model. As a result, the belt wear can be monitored by tracking the contact wheel revolutions per minute and the length of the belt. Other parameters such as the contact force can then be tweaked in order to factor for the difference in belt wear rate between the manual and robotic approach.

The table 1 below summarizes the benefits of using theoretical model versus an empirical model to determine the relationship between the depth of material removed and the surface finishing KPVs.

TABLE I. Theoretical vs Empirical Material Removal Model

No.	*Theoretical*	*Empirical*
Advantages		
1	Based on fundamental physical principles. Low cost.	Based on experimental data. Costly.
2	Wide range of applicability. (Freeform surfaces, different materials etc)	Applicable only to the range conducted in the experimental data.
3	Quick simulation and prediction of material removal.	New models for new products require long development by accumulating of trial data.
4	Predicted spatial material removal can be displayed visually with high resolution.	Generally only predicts constant material removal. Not possible to visualize.
Disadvantages		
1	Needs to be calibrated as not all parameters in the model are known	Do not require calibration as it is inherently based on actual data.
2	Cannot be applied for very fine, detailed shapes where contact pressure is unkown.	A new empirical model can be developed even for fine, detailed shapes

V. Conclusion

The new method is an enabler for robotic programmers, as it provides a whole package of quantitative information on the current manual process for the programmer to use in developing the robotic tool path strategy. This information includes visualization of the manual tool paths, features of the manual surface finishing process and their equivalent robotic surface finishing KPVs. In addition, expensive

robotic trials can be avoided as the relationship between the robotic KPVs and material removal depth can be determined directly from the manual process with the aid of a theoretical material removal model. Consequently, this method of capturing the manual surface finishing skill to program the industrial robot not only reduces the time taken to automate a manual process by enabling the robot programmer with a set of working KPVs from the start for further optimization, but also save on developmental costs by reducing the amount of consumables needed to develop a material removal model for the specific work piece.

The flow chart in Figure 9 shows a summary of the method described in the paper.

Figure 9. Flow Chart Summary

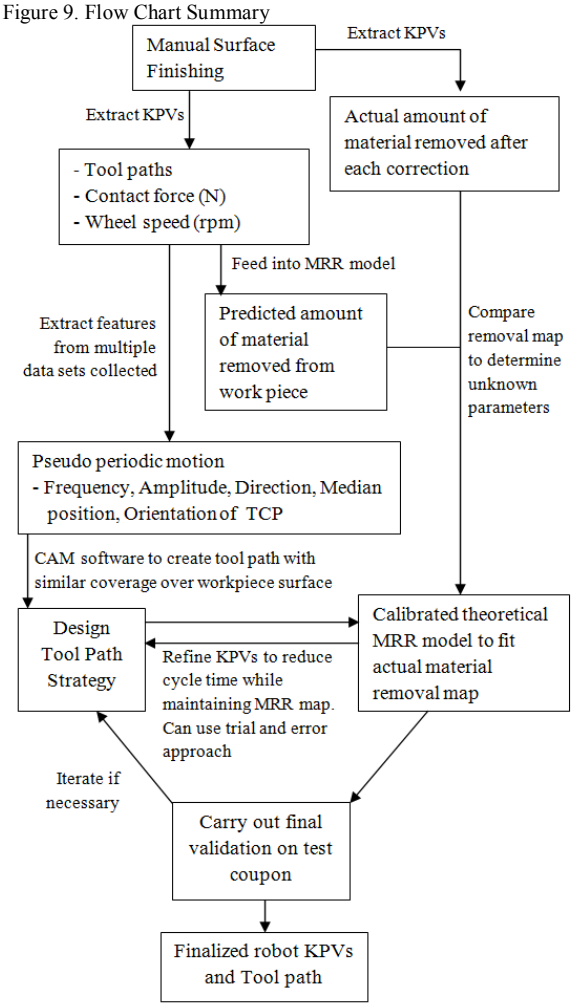

VI. FUTURE WORK

It is not feasible for the robot to follow the manual operator's tool paths exactly for more complex area material removal maps due to the fundamental difference between a robot and human. To overcome this problem, the robotic tool path planning will be done in a CAM software. The tool paths generated are structured robotic strategies (zig-zag paths that cover the entire material removal map area) which the robot can follow. Parameters of the generated tool path, such as the step over, can also be easily changed. In addition to determining the relationship of the depth of material removal to the KPVs, parameters such as the frequency, amplitude and direction of motion can also be extracted from the captured manual operator's tool path [8]. With the contact force and step over distance fixed, the feed rate can be adjusted [9] based on the calibrated analytical material removal model to ensure the same material removal map is generated as the manual operator. Given that all the input workpiece is within a certain tolerance, and that the captured manual material removal map has been proven to be the same for different workpieces and operators, the robotic strategy with the KPVs to generate the same removal map will also result in the grinding of the workpiece to geometrical conformance.

The novelty of this project is in showing that although the various manual operators may use very differing tool paths, velocities and forces to tackle the same grinding task, the skill of manual surface finishing can be encapsulated in the form of a material removal map. This can be proved in the future work, by carrying out KPV capture of various manual operators working on a certain finishing task. After capturing the KPVs of these manual operators, it will be fed into the analytical MRR model to calculate the material removal map. This material removal map would be similar to each other, even though the strategies of the manual operators may differ. This method of capturing and quantifying the surface finishing skill of a manual operator is novel and has not been previously carried out.

ACKNOWLEDGMENT

The authors wish to thank Dr Albert Causo for his help and advice in the research work.

REFERENCES

[1] H. Huang, Z. M. Gong, X. Q. Chen, and L. Zhou, "SMART robotic system for 3D profile turbine vane airfoil repair," *International Journal of Advanced Manufacturing Technology,* vol. 21, pp. 275-83, / 2003.

[2] L. Zhang, H. Y. Tam, C. M. Yuan, Y. P. Chen, and Z. D. Zhou, "An investigation of material removal in polishing with fixed abrasives," *Proceedings of the Institution of Mechanical Engineers, Part B: Journal of Engineering Manufacture,* v216, n1, pp. 103-112, 2002.

[3] H.-y. Tam and H. Cheng, "An investigation of the effects of the tool path on the removal of material in polishing," *Journal of Materials Processing Technology,* vol. 210, pp. 807-818, 3/19/ 2010.

[4] L. Zhang, H. Y. Tam, C. M. Yuan, Y. P. Chen, Z. D. Zhou, and L. Zheng, "On the removal of material along a polishing path by fixed abrasives," *Proceedings of the Institution of Mechanical Engineers, Part B: Journal of Engineering Manufacture,* vol. 216, pp. 1217-1225, 2002.

[5] X. Ren, M. Cabaravdic, X. Zhang, and B. Kuhlenkotter, "A local process model for simulation of robotic belt grinding," *International Journal of Machine Tools & Manufacture,* vol. 47, pp. 962-70, 05/ 2007.

[6] R. Xiangyang and B. Kuhlenkotter, "Real-time simulation and visualization of robotic belt grinding processes," *International Journal of Advanced Manufacturing Technology,* vol. 35, pp. 1090-9, 02/ 2008.

[7] S. Wu, K. Kazerounian, Z. Gan, and Y. Sun, "A simulation platform for optimal selection of robotic belt grinding system parameters," *International Journal of Advanced Manufacturing Technology,* vol. 64, pp. 447-458, 2013.

[8] A. Irish, I. Mantegh, and F. Janabi-Sharifi, "A PbD approach for learning pseudo-periodic robot trajectories over curved surfaces," in *Advanced Intelligent Mechatronics (AIM), 2010 IEEE/ASME International Conference on*, 2010, pp. 1425-1432.

[9] H. Y. Tam, C. K. A. Mok, and K. L. Yiu, "Tool Dwell Time Computation in Computer-controlled Surfacing based on Constrained Optimization," *Machining Science and Technology*, 13(3) pp. 356-371, 2009